RSC Advances

This article can be cited before page numbers have been issued, to do this please use: S. A. Khan, A. M. Asiri and S. H. Al-Thaqafy1, *RSC Adv.*, 2016, DOI: 10.1039/C6RA02814D.

ROYAL SOCIETY OF CHEMISTRY

www.rsc.org/advances

View Article Online
DOI: 10.1039/C6RA02814D

Optical properties and fluorescence quenching of biological active ethyl 4-(4-N,N-dimethylamino phenyl)-2-methyl-5-oxo-4,5-dihydro-1*H*-indeno[1,2-*b*]pyridine-3-carboxylate (DDPC) dye as probe to determine CMC of surfactants

Salman A. Khan[1,*], Abdullah M. Asiri[1,2], Saad H. Al-Thaqafy[1],

[1]Chemistry Department, Faculty of Science, King Abdulaziz University, P.O. Box 80203, Jeddah 21589, Saudi Arabia

[2]Center of Excellence for Advanced Materials Research (CEAMR), King Abdulaziz University, P.O. Box 80203, Jeddah 21589, Saudi Arabia

*Author to whom correspondence should be addressed; e-mail: *sahmad_phd@yahoo.co.in*.

Abstract 4-(4-N,N-dimethylamino-phenyl)-2-methyl-5-oxo-4,5-dihydro-1*H*-indeno[1,2-*b*]pyridine-3-carboxylate (DDPC) was prepared by multi component reaction of indane-1,3-dione with 4-(dimethylamino)benzaldehyde, ethyl acetoacetate and ammonium acetate. Data obtained from FT-IR, ^{1}H-NMR, ^{13}C-NMR, EI-MS and elemental analysis were consistent with chemical structure of newly prepared DDPC. Electronic absorption and emission spectrum of DDPC have been measured in different solvents. DDPC dye exhibits red shift in emission spectrum as solvent polarity increases, indicating a large change in dipole moment of DDPC molecule upon excitation due to intramolecular charge transfer in excited DDPC. Excited state intermolecular hydrogen bonding affect on the energy of emission spectrum and fluorescence quantum yield of DDPC molecule. DDPC dye undergoes solubilization in different micelles and may be used as a probe to determine the critical micelle concentration (CMC) of SDS and CTAB. DDPC dye can also use as probe of the polarity and hydrogen bonding properties of its local microenvironment**.** The anti-bacterial activity of the DDPC was first tested *in vitro* by the disk diffusion assay against two Gram-positive and two Gram-negative bacteria, and then the

View Article Online
DOI: 10.1039/C6RA02814D

minimum inhibitory concentration (MIC) was determined with the reference of standard drug Tetracycline.

Keywords: DDPC, Stokes shift, Oscillator strength, Dipole moment, fluorescence quantum yield, Micellization

View Article Online
DOI: 10.1039/C6RA02814D

Introduction

Heterocyclic compound with the especial references of pyridine occupy special place and have attracted considerable attention because of their broad pharmacological activities, including anti-bacterial, anti-tumor, anticancer,[1-3] antiviral, [4] anti-inflammatory, [5] antimicrobial, [6] anti-diabetic, [7] antihypertensive [8] and osteogenic activities, [9] in addition to treatment of CNS disorders. [10] Various synthetic methods have been reported for the synthesis of pyridine derivative, bi-cyclic heterocyclic compounds such as pyrazolo-pyridine, thiazolo-pyridine, triazolo-pyridine have synthesized by the cyclization of pyridine. [11] It's also used as ligands for the metal complexes by the coordinate with the transition metal complexes. [12] Due to presence of long π bond conjugation system in pyridine derivative its also used in the felids of martial science such as nonlinear optical properties, [13] photonic materials, [14] devices, optical limiting,[15] electrochemical sensing, [16] light-emitting devices, [17] langmuir film, [18] and solar cell materials. [19] However, the pyridine has been used extensively for the photo-alignment and photo-crosslinking unit in polymers. Physicochemical characteristics, such as, solvatochromic, piezochromic, oscillator strength, dipole moment, fluorescence quantum yield and photostability, are also most important studies for determining the physical behavior of compounds. [19] Donor (D) -π -acceptor (A) long π bond conjugate system gives the good physicochemical behavior due to the intramolecular charge transfer by π-bond from the donor group to acceptor group. [20] On the basis of literature survey we find that lot of work have been done on chromophores,[21] to the best of our knowledge their is not much deep investigation on the prescient topic which we are reporting first time, therefore due to the possible importance of the D -π -A chromophores our interest in the development of heterocycle -based D -π -A chromophores. In the present study, we wish to report the

View Article Online
DOI: 10.1039/C6RA02814D

synthesis of new heterocycle-based chromophore. One-pot multicomponent reactions (MCR) have conventional significant attention in synthetic chemistry as they can produce target products from readily available starting materials in one reaction step without isolating the intermediates thus reducing reaction times, labor cost, and waste production. [22] Therefore in the present paper we are reporting the synthesis of 4-(4-N,N-dimethylamino-phenyl)- 2 - methyl - 5- oxo - 4, 5-dihydro-1*H*-indeno [1,2-*b*] pyridine-3 carboxylate (DDPC) by MCR and physicochemical studies such as oscillator strength, dipole moment, fluorescence quantum yield, fluorescence quenching in organized media. DDPC dye undergoes solubilization in different micelles and used as a probe to determine the critical micelle concentration (CMC) of SDS and CTAB .

Experimental

Apparatus

FT-IR spectra were recorded on a Nicolet Magna 520 FT-IR spectrometer. ^{1}H-NMR and ^{13}C-NMR experiments were performed in $CDCl_3$ on a Brucker DPX 600 MHz spectrometer using tetramethyl silane (TMS) as internal standard at room temperature. Melting points were recorded on a Thomas Hoover capillary melting apparatus without correction. UV-Vis electronic absorption spectra were acquired on a Shimadzu UV-1650 PC spectrophotometer. Absorption spectra were collected using a 1 cm quartz cell. Steady state fluorescence spectra were measured using Shimadzu RF 5301 PC spectrofluorophotometer with a rectangular quartz cell. Emission spectra were monitored at right angle. All fluorescence spectra were blank subtracted before proceeding in data analyses.

Chemicals and reagents

View Article Online
DOI: 10.1039/C6RA02814D

The appropriate chemical indane-1,3-dione, 4-(dimethylamino)benzaldehyde, ethyl acetoacetate and ammonium acetate was purchased from Acros Organic. Other reagents and solvents (A.R.) were obtained commercially and used without further purification, except dimethylformamide (DMF), ethanol and methanol.

4-(4-N,N-dimethylamino phenyl)-2-methyl-5-oxo-4,5-dihydro-1H-indeno[1,2-b]pyridine-3-carboxylate (DDPC)

To an alcoholic solution (50 mL) of indane-1,3-dione 2 (0.01 mol), 4-(dimethylamino)benzaldehyde (0.01 mol), ethyl acetoacetate 3 (0.01 mol), ammonium acetate (0.02 mol) and a drop of piperidine were added and the mixture was refluxed for 2 h. The reaction mixture was concentrated to half of its original volume and allowed to cool in an ice-chest. The solid thus separated was filtered, washed with ice cold aqueous ethanol and crystallized from petroleum ether (60–80°C)-chloroform (1: 1) (Scheme 1).

Dark Brown solid: m.p. 122° C; EIMS *m/z* (rel. int.%): 391 (72) $[M + 1]^+$; IR (KBr) ν_{max} cm^{-1}: 3254 (N-H), 2964 (C-H), 1656 (C=O), 1585 (C=C); 1246 (C-N); ^{1}H NMR (600 MXz $CDCl_3$) (δ/ppm): 9.16 (s, NH), 8.51- 6.47 (m, 9H, CH aromatic) 4.07 (s, 3H, -CH_3), 4.00 (s, 3H, -CH_3), 3.96 (s, 3H, -CH_3), 3.85-3.75 (q, CH_2-CH_3), 1.61 (t, -CH_2-CH_3); ^{13}CNMR ($CDCl_3$) δ: 168.22 (C=O), 156.25 (pyridine C), 139.91, 134.76, 134.61, 124.81, 122.86, 122.78 (Ar-C). Anal.calc. for $C_{24}H_{24}N_2O_3$: C, 74.21, H, 6.23; N, 7.21 Found: C, 74.18, H, 5.97, N, 6.16.

View Article Online
DOI: 10.1039/C6RA02814D

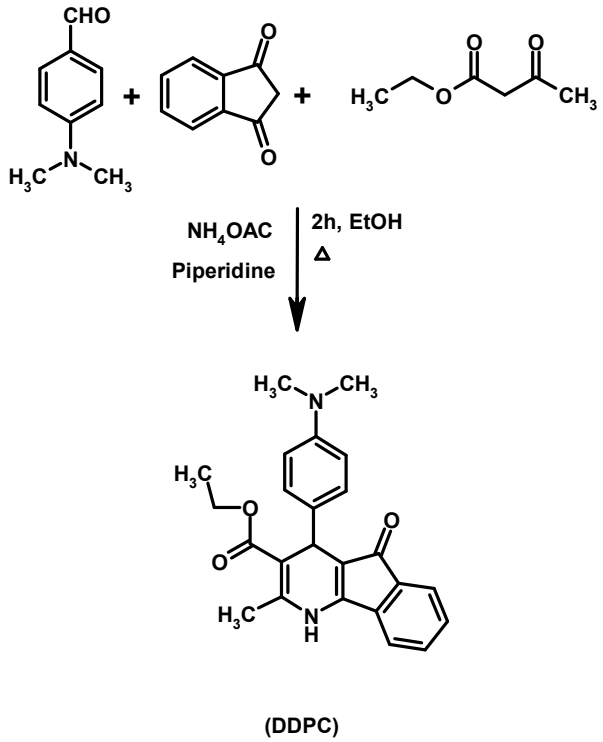

(DDPC)

Scheme 1: Synthesis of DDPC

The fluorescence quantum yield (ϕ_f) of DDPC (1 x 10^{-5} M) was evaluated in different solvents. Rhodamine 6G (1 x 10^{-5} M) in ethanol (ϕ_f = 0.94)) was selected as a standard sample since rhodamine 6G absorbs using the same excitation wavelength (λ_{ex} = 385 nm) of DDPC in ethanol and same concentration of the solution DPPC and rhodamine 6G) to obtain the absorption spectra. [23] It is, therefore, expected that the same number of photons are absorbed by both samples (Rhodamine 6G and DDPC). The fluorescence quantum yield of DDPC can be related to that of the standard by the following relationship: [24]

$$\Phi = \Phi_r \frac{I\ x\ A_r\ x\ n^2}{Ir\ x\ A\ x\ n^2{}_r} \qquad (1)$$

View Article Online
DOI: 10.1039/C6RA02814D

Where ϕ is the quantum yield, I is the integrated emission intensity, A is the absorbance at excitation wavelength, and n is the refractive index of the solvent. The subscript r refers to the reference fluorophore of known quantum yield.

Organism culture and in vitro screening

Antibacterial activity was 4-(4-N,N-dimethylamino phenyl)-2-methyl-5-oxo-4,5-dihydro-1H-indeno[1,2-b]pyridine-3-carboxylate (DDPC) done by the disk diffusion method with minor modifications. *S. aureus, S. pyogenes, S. typhimurium* and *E. coli* were sub-cultured in BHI medium and incubated for 18 h at 37 ºC, and then the bacterial cells were suspended, according to the McFarland protocol in saline solution to produce a suspension of about 10^{-5} CFU mL^{-1}: 10 µL of this suspension was mixed with 10 mL of sterile antibiotic agar at 40 ºC and poured onto an agar plate in a laminar flow cabinet. Five paper disks (6.0 mm diameter) were fixed onto nutrient agar plate. 1mg of DDPC was dissolved in 100 µL DMSO to prepare stock solution to form different concentration 10, 20, 25, 50, and 100 µg/µL of DDPC different concentration were poured over disk plate on to it. Tetracycline (30 µg/disk) was used as standard drug (positive control). DMSO poured disk was used as negative control. The susceptibility of the bacteria to the DDPC was determined by the formation of an inhibitory zone after 18 h of incubation at 36 ºC (Table **2**) reports the inhibition zones (mm) of DDPC and the controls. The minimum inhibitory concentration (MIC) was evaluated by the macro dilution test using standard inoculums of 10^{-5} CFL mL^{-1}. Serial dilutions of the DDPC, previously dissolved in dimethyl sulfoxide (DMSO) were prepared to final concentrations of 512, 256, 128, 64, 32, 16, 8, 4, 2 and 1 µg/ mL to each tube was added 100µL of 24 h old inoculum. The MIC defined as the lowest concentration of the DDPC which inhibits the visible growth after 18 h was determined visually after incubation for 18 h at 37 ºC and the

View Article Online
DOI: 10.1039/C6RA02814D

results are presented in table 2. Tests using DMSO and tetracycline as negative and positive controls were also performed.

Results and discussion

Chemistry

4-(4-N,N-dimethylamino-phenyl)-2-methyl-5-oxo-4,5-dihydro-1*H*-indeno[1,2-*b*]pyridine-3-carboxylate (DDPC) was prepared by multi component reaction of indane-1,3-dione with 4-(dimethylamino)benzaldehyde, ethyl acetoacetate, ammonium acetate. [25] The purified dye was characterized by the FT-IR, ^{1}H-NMR, ^{13}C-NMR, EI-MS m/z (rel. int.%), and elemental analysis. FT-IR spectra of DDPC show that a characteristic band at 1676 cm^{-1} of the ν (C=O) peak for indane-1,3-dione that is shifted to a lower frequency of 1656 cm^{-1} for DDPC. This is due to the one C=O is utilized for the formation of pyridine. The IR spectrum of DDPC shows the characteristic band at 3254 cm^{-1} due to presence –NH group. IR spectra shows sharp peak at 1246 cm^{-1} due presence of C-N-C stretch which is conform to formation of pyridine ring. The ^{1}H-NMR spectra of DDPC measured at room temperature shows one singlet at 9.16 ppm for the NH. The appearance of multiplets at δ 8.51- 6.47 was due to aromatic protons and three singlet at δ 4.07, 4.00 and 3.96 for corresponding to the three methyl group present in the DDPC. Moreover, ^{13}C NMR ($CDCl_3$) spectra of DDPC was recorded in $CDCl_3$ and spectral signals are in good agreement with the probable structures. The carbonyl carbon of the DDPC usually appears at δ 168.22 in it ^{13}C NMR spectrum. ^{13}C-NMR spectra showed signals in the range of δ 139.91-122.78 ppm due to aryl carbon. Details of ^{13}C-NMR spectra of DDPC are given in the experimental section. Finally characteristic peaks were observed in the mass spectra of DDPC. The mass spectrum of DDPC shows a molecular ion peak ($M^{+\cdot}$) m/z 391.

View Article Online
DOI: 10.1039/C6RA02814D

Spectral behavior of DDPC in different media

UV-vis absorption spectra of the DDPC (1 x 10^{-5} M) was measured in various non-polar, polar aprotic and polar protic solvents such as ethanol, methanol, dimethylsulfoxide, dimethylformamide, chloroform, dichloromethane, carbon tetrachloride, acetonitrile, dioxan, tetrahydrofuran. Fig 1 shows absorption spectra of a1 x10^{-5} mol dm^{-3} solution of DDPC in these solvents as a sample. As it can be seen from Fig 1, in the all solvent tested the main band of DDPC, located in the spectral range 371-400 nm. Shorter wavelength band in UV region observed for studies DDPC in different solvent system is assigned to π to π^* transition of the benzenoid system toward the other ring which is characterized by high electron donation and electron accepting character present in its structure. On excitation at 385 nm and the range of λ of emission between 395 nm to 700 nm, the emission spectrum of DDPC (1 x 10^{-5} M) shows smooth correlation with increasing polarities of the solvent, broad and red shifted (Fig 2 & Table 1) as the solvent polarity increases. The red-shift from 475 nm in CCl_4 to 548 in DMSO indicates that photoinduced intramolecular charge transfer (ICT) occurs in the singlet excited state and therefore the polarity of DDPC increases on excitation. [26] The red shift of the fluorescence peak in alcoholic solvents are assigned to solute – solvent hydrogen bonding interaction in the singlet excited state which causes red shift in the observed spectra (Table 1). [27]

A simplified description of hydrogen bonding of DDPC is shown in Scheme 2. Type (a) hydrogen bonding is strengthened in the excited state, since the charge density at the carbonyl oxygen is enhanced in the ICT excited state. On the other hand, type (b) hydrogen bonding is weakened on photoexcitation, because the charge densities at the N-$(CH_3)_2$ decrease in the excited state.

View Article Online
DOI: 10.1039/C6RA02814D

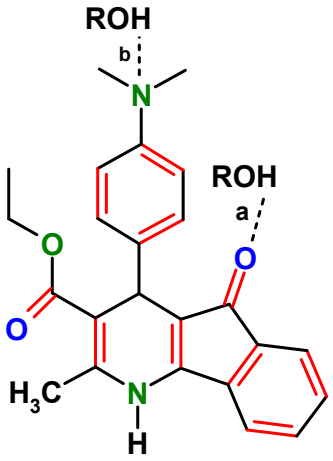

Scheme 2 : Type of hydrogen bonding of DDPC

The energy of absorption (E_a) and emission (E_f) spectra of the DDPC in different solvents correlated with the empirical Dimroth polarity parameter E_T (30) of the solvent (Fig. 3). [28] A linear correlation between the energy of absorption and emission versus polarity of solvents was obtained (Equation 2 and 3), implying potential application of these parameters to probe the microenvironment of DDPC.

$$E_a = 75.17 - 0.1032 \times E_T (30) \quad (2)$$

$$E_f = 68.28 - 0.257 \times E_T (30) \quad (3)$$

Analysis of solvatochromic behavior allows estimating the difference in the dipole moment between the excited and ground states ($\Delta\mu_e$- $\Delta\mu_g$). This was achieved by applying the simplified Lippert – Mataga equation (4, 5). [29]

View Article Online
DOI: 10.1039/C6RA02814D

$$\Delta \bar{\nu}_{st} = \frac{2(\mu_e - \mu_g)^2}{hca^3}\Delta f + Const. \quad (4)$$

$$\Delta f = \frac{k-1}{2k+1} - \frac{n^2-1}{2n^2+1} \quad (5)$$

Where Δυ is the Stokes shift which increases with increase in the solvent polarity to pointing to stronger stabilization of singlet excited state in polar solvent, h is Planck constant, c is the speed of light and a is the Onsager cavity radius, k and n are the dielectric constant and refractive index of the solvent, respectively. The constant represents higher order terms which are usually neglected. The Onsager cavity radius was taken as 5.7 Å. [30] Fig 4 shows the plot of Stokes shift versus the orientation polarizability (Δf). The changes of dipole moment (Δμ) upon excitation was calculated from slope of the plot and the cavity radius is Δμ = 5.58 Debye. This change in dipole moment is caused by redistribution of atomic charges in the excited state as a result of charge transfer from the electron rich –N-$(CH_3)_2$ group to electron acceptor keto-group fragment.

The oscillator strength ($\boldsymbol{f}$) and transition dipole moment (μ_{12}) of electronic transition for DFTP from ground to excited singlet state ($S_o \rightarrow S_1$) was calculated in different solvents using the following equation (6, 7). [31]

$$f = 4.32\times10^{-9}\int \varepsilon(\bar{\nu})\, d\bar{\nu} \quad (6)$$

$$\mu_{12}{}^2 = \frac{f}{4.72\times10^{-7}\, E_{max}} \quad (7)$$

View Article Online
DOI: 10.1039/C6RA02814D

Where ε the numerical value for molar decadic extinction coefficient is measured in $dm^3\ mol^{-1}cm^{-1}$ and υ is the value of wavenumber measured in cm^{-1} and E_{max} is the energy maximum of absorption band in cm^{-1}. The values of f and (μ_{12}) are listed in Table 1 and indicates that the $S_o \rightarrow S_1$ is strongly allowed transition

The empirical Dimroth polarity parameter, E_T (30) and E_T^N of DDPC was also calculated according to the following equation. [32, 33]

$$E_T^N = \frac{E_T(solvent) - 30.7}{32.4} \quad (8)$$

$$E_T(solvent) = \frac{28591}{\lambda_{max}} \quad (9)$$

where λ_{max} corresponds to the peak wavelength (nm) in the red region of the intramolecular charge transfer absorption of DDPC. The red (bathochromic) shift from CCl_4 to DMSO indicates that photoinduced intramolecular charge transfer (ICT) occurs in the singlet excited state, and the polarity of DDPC, therefore, increases on excitation.

Fluorescence quantum yield

The fluorescence quantum yield (ϕ_f) of DDPC depends strongly on the solvent properties (Table 1). The fluorescence quantum yield can be correlated with $E_T(30)$ of the solvent, where $E_T(30)$ is the solvent polarity parameter introduced by Reichardt.[34] The fluorescence quantum yield of DDPC increases with increasing solvent polarity from 0.16 in a non-polar solvent CCl_4 to 0.43 in a moderately polar solvent dioxan; with a further increase in solvent polarity the fluorescence quantum yield seems to decrease, i.e., 0.29 in a strongly polar solvent, DMSO. This indicates the occurrence of negative solvatokinetic effect and positive solvatokinetic effect during the course

View Article Online
DOI: 10.1039/C6RA02814D

of increasing solvent polarity. [35] One main reason for the negative solvatokinetic effect (increase ϕ_f with a suitable enhancement of ICT) could be due to the biradicaloid charge transfer involving the un-bridged double bonds and the other cause could be related to the proximity effect for compounds with n-л and л-л* electron configuration. In other words, in non-polar solvents, these effects will result in effective nonradiative decay of the excited states. In strong polar solvents, the fluorescence quantum yield decreases, due to large degree of intramolecular charge transfer, which causes an increase in the rate of radiationless relaxation of an excited state, giving rise to positive solvatokinetic effect (reduction in ϕ_f by strong ICT). Moreover, the much lower fluorescence quantum yields in proton solvents can be attributed to the hydrogen bond interaction between the molecule and surrounding solvent, which results in an additional nonradiative decay as observed in other dipolar molecules.

Effect of surfactant on emission spectrum of DDPC

The emission spectrum of 1 x 10^{-5} mol dm^{-3} of DDPC has also measured in cationic micelle cetyltrimethyl ammonium bromide (CTAB) and anionic micelle sodium dodecyl sulphate (SDS). As shown in Fig 6 and Fig 7, the emission intensity of DDPC increases with increasing the concentration of surfactant, an abrupt change in fluorescence intensity is observed at surfactant concentration of 7.30 x$10^{-4}$and 7.45 x 10^{-3} mol dm^{-3}, We have used Carpena's method [36] to obtain the value of cmc from the data of emission intensity and found the same cmc value shown in Fig. 6 and Fig. 7 as swhich are very close to the critical micelle concentration of CTAB and SDS, [37] thus DDPC can be employed as a probe to determine the CMC of a surfactants. It was well known that aromatic molecules were generally solubilized in the palisade layer of micelle. [38, 39] Thus the enhancement of emission intensity is attributed to the passage

View Article Online
DOI: 10.1039/C6RA02814D

of dye molecule from the aqueous bulk solution to the palisade layer of micelle. The decrease in polarity of the microenvironment around dye molecule results in the reduction of non-radiative rate from ICT state to low-laying singlet or triplet state due to the enlargement the energy gap between them, which leads to an increase in emission intensity. Critical micelle concentration (CMC) of SDS and CTAB with DDPC were further conformed by the conductometric method.

Fluorescence quenching of DDPC with alcoholic solvents

The fluorescence quenching of DDPC in dioxan (On excitation at 385 nm) (λ_{ex} = 385 nm) was studied by using different concentration of some polar protic solvents of different acidity, such as methanol, ethanol, 2-propanol and butanol as quenchers Figure 8(a)-11 a). As follows from these figures, the fluorescence spectra undergo very complex changes on adding different concentration of alcoholic solvents , i.e., they are shifted to longer wavelength, possess changed half widths and band profiles of the emission spectrum. This behavior indicates, that in such a solution an extra factor contributes to the well known dipole-dipole interaction, i.e., hydrogen-bonding interactions between the DDPC with the alcohol. [40] The Stern–Volmer constants (K_{SV}) were calculated from the Stern– Volmer plots shown in Fig 8(b)- 11(b). The K_{SV} constant was determined as 0.206, 0.169, 0.99 and 0.094 M^{-1} in methanol, ethanol, 2-propanol and butanol respectively, which increases according to the acidity (α) of the alcohol. It seems that the K_{SV} value in case of methanol is higher than that in the other solvents, which indicates that the possibility of hydrogen bonding with solute increases with the decreeing the number of carbon atoms in the solvent molecule. The dependence of fluorescence characteristics on solvent properties imply a potential application of DDPC to probe of the polarity and hydrogen bonding properties of it local microenvironment.

View Article Online
DOI: 10.1039/C6RA02814D

$$I_0 / I_f = 1 + K_{sv}[Q] \quad (10)$$

where I_o and I_f are the relative integrated fluorescence intensities without and with the quencher concentration [Q] and K_{sv} (Stern-Volmer constant).

Antibacterial activity

Disc-diffusion assay

4-(4-N,N-dimethylamino-phenyl)-2-methyl-5-oxo-4,5-dihydro-1H-indeno[1,2-b]pyridine-3-carboxylate (DDPC) was tested for their antibacterial activities by disc-diffusion method using nutrient broth medium [contained (g/L): beef extract 3 g; peptone 5 g; pH 7.0. [41] The Gram-positive bacteria and Gram-negative bacteria utilized in this study are *S. aureus, S. pyogenes, S. typhimurium and E. coli*. In the disc-diffusion method, sterile paper discs (0.5 mm) impregnated with DDPC dissolved in dimethylsulfoxide (DMSO) at concentration 100 μg/mL were used. Then, the paper discs impregnated with the solution of the test DDPC were placed on the surface of the media inoculated with the microorganism. The plates were incubated at 35 ^{o}C for 24 h. After incubation, the growth inhibition zones are shown in table 2.

Assessment of minimum inhibitory concentration (MIC)

The MIC of synthesized DDPC and standard drug were investigated against two gram positive and two gram negative bacteria using broth dilution method (BDM). The data is reported as MIC which is defined as the lowest concentration required to inhibit 90% growth in comparison to control (absence of DDPC) for each isolate. Table 2 summarizes the *in vitro* susceptibilities of both the types of isolates against DDPC. Evaluation of MIC showed that DDPC active *in vitro* against all the tested

View Article Online
DOI: 10.1039/C6RA02814D

microorganisms with varying degrees of inhibition, within the reference range.

Conclusion

Novel donor, accepter heterocyclic chromophore (4-(4-N,N-dimethylamino-phenyl)-2-methyl-5-oxo-4,5-dihydro-1*H*-indeno[1,2 *b*]pyridine-3-carboxylate) (DDPC) was prepared by multi component reaction of indane-1,3-dione with 4-(dimethylamino)benzaldehyde, ethyl acetoacetate, ammonium acetate and characterized by various spectral techniques. Optical properties of DDPC dye including singlet absorption, extinction coefficient, stokes shift, oscillator strength, dipole moment and fluorescence quantum yield were investigated on the basis of the polarity of solvent. The absorption and emission spectra of DDPC exhibit an intramolecular charge transfer band; which showed a positive solavotochromism in different solvents. The emission spectra of the DDPC also reveal the intramolecular charge transfer band character. These findings confirm that there is a significant electron transfer between the donating moiety and the accepting fragment through the π conjugated. DDPC dye undergoes solubilization in different micelles and may be used in the determination of CMC of surfactants (SDS and CTAB). DDPC dye can also use as probe of the polarity and hydrogen bonding properties of its local microenvironment. The antibacterial activity of DDPC was examined using cultures of bacteria and the results showed that DDPC showed better antibacterial activity for both types of the bacteria (Gram-positive and Gram-negative) as compared to reference drug tetracycline.

Acknowledgments

The authors are thankful to the Chemistry Department at King Abdulaziz University for providing research facilities.

View Article Online
DOI: 10.1039/C6RA02814D

References

1. B. K. Srivastava, M. Solanki, B. Mishra, R. Soni, S. Jayadev, D. Valani, M. Jain, P. R. Patel, *Bioorg. Med. Chem. Lett.,* 2007, **17,** 1924.
2. Y. Jiao, B. Xin, Y. Zhang, X. Wu, X. Lu, Y. Zheng, W. Tang, X. Zhou, *Eur. J. Med. Chem.,* 2015, **90,** 170.
3. M. H. Helal, S. A. El-Awdan, M. A. Salem, T. A. Abd-elaziz, Y. A. Moahamed, A. A. El-Sherif, G. A. M. Mohamed, *Spectrochemica Acta A:* 2015, **135**, 764.
4. S. Musiu, G. Purstinger, S. Stallinger, R. Vrancken, A. Haegeman, F. Koenen, P. Leyssen, M. Froeyen, J. Neyts, J. Paeshuyse, *Antiviral Res.,* 2014, **106,** 71.
5. R. M. Mohareb, M. Y. Zaki, N. S. Abbas, *Steroids,* 2015, **98,** 80.
6. G. Jose, T. H. S. Kumara, G. Nagendrappa, H. B. V. Sowmya, J. P. Jasinski, S. P. Millikan, S. S. More, B. Janardhan, B. G. Harish, N. Chandrika, *J. Mol. Struct.* 2015, **1081**, 85.
7. P. P. Dixit, T. P. A. Devasagayam, S. Ghaskadbi**,** *Eur. J. Pharmacol.,* 2008, **581,** 216.
8. M. Abdallah, I. Zaafarany, S. O. Al-Karanee, A. A. El-Fattah*, Arabian J. Chem.,* 2012, **5,** 225.
9. P. Dixit, M. P. Khan, G. Swarnkar, N. Chattopadhyay, R. Maurya, *Bioorg. Med. Chem. Lett.,* 2011, **21,** 4617.
10. C. B. Mishra, S. Kumari, M. Tiwari, *Eur. J. Med. Chem.,* 2015, **92,** 1
11. D. Zhu, X. Chen, R. Huang, S. Yan, J. Lin, *Tetrahedran,* 2015, **71,** 2363.
12. V. Duros, H. Sartzi, S. J. Teat, Y. Sanakis, O. Roubeau, S. P. Perlepes, *Inorg. Chem. Commun.,* 2014, **50,** 117.
13. A. P. Menezes, A. Jayarama, S. W. Ng, *J. Mol. Struct.,* 2015, **1088,** 85.

View Article Online
DOI: 10.1039/C6RA02814D

14. C. S. Stanm, C. Peptu, N. Marcotte, P. Horlescu, D. Sutiman, *Inorg. Chim. Acta.,* 2015, **429,** 160

15. S. Guang, S. Yin, H. Xu, W. Zhu, Y. Gao, Y. Song, *Dyes & Pigm.,* 2007, **73,** 285.

16. D. Liaw, K. Wang, S. P. Pujari, Y. Huang, B. Tao, M. Chen, K. Lee, J. Lai, *Dyes & Pigm.* 2009, **82,** 109.

17. Y. Z. Wang, D. D. Gebler, D. K. Fu, T. M. Swager, A. G. MacDiarmid, A. J. Epstein, *Synth. Met.* 1997, 85, 1179.

18. M. Suzuki, Thin Solid Films, 1989, **180,** 253.

19. W. Ying, X. Zhang, X. Li, W. Wu, F. Guo, J. Li, H. Agren, J. Hua, *Terahedron,* 2014, **70,** 3901.

20. H. M. Marwani, A. M. Asiri, S. A. Khan, Spectral, stoichiometric ratio, physicochemical, polarity and photostability studies of newly synthesized chalcone dye in organized media, *J Lumin.,* 2013, **136,** 296.

21. S. K. Lanke, N. Sekar, *J Photochem. Photobio A:* 2016, **321**, 63-71.

22. K. Ablajan, W. Kamil, A. Tuoheti, S. Wan-Fu, *Molecules,* 2012, **17,** 1860-1869.

23. S. A. El-Daly, A. M. Asiri, A. Y. Obeid, S. A. Khan, K. A. Alamry, M. A. Hussien, G. A. Al-Sehemi, *Opt Laser Technol.,* 2013, **45,** 605.

24. S. A. El-Daly, A. M. Asiri, S. A. Khan, K. A. Alamry, *J. Lumin.,* 2013, **134,** 819.

25. R. Pandian, E. Naushad, V. Vijayakumar, G. H. Peters, P. M. Nanjappagounder, *Chem Cent J* 2014, **8,** 1-7

26. R. Frolicker, *J. Phys. Chem. A:* 2002, **106,** 1708.

27. S. Suppan, *J. Photochem. Photobiol. A:***,** 1990, **50,** 293.

View Article Online
DOI: 10.1039/C6RA02814D

28. N. Mataga, T. Kubota, Molecular interaction and electronic spectra, New York, Marcel Dekker, 1970, 371.

29. M. Gaber, S. A. El-Daly, T. A. Fayed, Y. S. El-Sayed, *Opt. Laser Technol.,* 2008, **40,** 528.

30. C. Reichardt, Solvents and Solvent Effects in Organic Chemistry, 2nd ed., VCH, Weiheim, 1988: 359.

31. C. Reichardt, C.: Solvents and solvent effects in organic chemistry, 2 nd ed. Weiheim: VCH, 1988 p.35.

32. N. J. Turro, Molecular photochemistry (frontiers in chemestry), 1st ed., W. A. Benjamin, Inc., Reading, MA, 286 (1965)

33. B. J. Coe, J. A. Harris, I. Asselberghs, K. Clays, G. Olbrechts, A. Persoons, J. T. Hupp, R. C. Johnson, S. J. Coles, M. B. Hursthouse, K. Nakatani, *Adv. Funct. Mater.* 2002, **12,** 110.

34. K. Rurack, M. L. Dekhtyar, J. L. Bricks, U. Resch-Genger, W. Retting, *J. Phys. Chem. A* 1999, **103,** 9626.

35. R. Gahlaut, N. Tewari, J. P. Bridhkoti, N. K. Joshi, H. C. Joshi, S. Pant, *J. Mol. Liq.,* 2011, **161,** 141.

36. P. Carpena, J. Aguiar, P. Bernaola-Galvan, and C. C. Ruiz, *Langmuir* 2002, **18,** 6054-6058**.**

37. S. A. El-Daly, A. M. Asiri, K. A. Alamry, A. Y. Obaid, *J. Lumin.,* 2013, **139,** 69.

38. K. N. Ganesh, P. Mitra, D. Balasubramanian, *J. Phys. Chem.* 1982, **86,** 4291.

39. K. A. Dill, D. E. Koppel, R. S. Cantor, J. D. Dill, D. Bendouch, S. H. Chen, *Nature,* 1984, **309,** 42.

40. W. Kirk, W. Wessels, *Biophys. Chem.,* 2007, **125,** 32.

View Article Online
DOI: 10.1039/C6RA02814D

41. S. A. Khan, A. M. Asiri, K. Sharma, *Med. Chem. Res.,* 2013, **22,** 1998.

View Article Online
DOI: 10.1039/C6RA02814D

Table 1: Spectral data of DDPC in different solvents

Solvent	Δf	E_T^N	E_T (30) Kcal mol^{-1}	λ_{ab}(nm)	λ_{em}(nm)	ε $M^{-1}cm^{-1}$	f	μ_{12} Debye	$\Delta\bar{\nu}$ (cm^{-1})	Φ_f
EtOH	0.305	1.28	72.38	395	559	8410	0.24	4.48	7427	0.092
DMSO	0.266	1.25	71.47	400	548	11480	0.31	5.12	6752	0.29
MeOH	0.308	1.32	73.49	389	561	8073	0.25	4.53	7881	0.035
DMF	0.263	1.35	74.26	385	540	9590	0.28	4.77	7396	0.33
$CHCl_3$	0.217	1.35	74.65	383	532	9158	0.26	4.59	7313	0.44
CH_2Cl_2	0.255	1.33	73.87	387	530	7810	0.21	4.14	6972	0.40
Acetonitrile	0.274	1.38	75.43	379	542	9183	0.29	4.82	7935	0.30
Dioxan	0.148	1.41	76.65	373	490	11840	0.30	4.86	6401	0.43
THF	0.263	1.41	76.44	374	497	8614	0.22	4.17	6617	0.34
CCl_4	0.024	1.43	77.06	371	475	9752	0.23	4.25	5902	0.16

Table 2. Antibacterial activity of DDPC positive control: Tetracycline and negative control (DMSO) measured by the Halo Zone Test (Unit, mm) and MIC.

	Corresponding effect on microorganisms			
	A. hydrophila	*Y. enterocolitica*	*L. monocytogenes*	*P. aeruginosa*
DDPC (Disc)	11.4 ± 0.3	12.5 ± 0.5	14.3 ± 0.2	15.2 ± 0.2
DDPC (MIC)	64	64	32	32
Tetracycline (Disc)	13.0 ± 0.5	20.0 ± 0.5	12.0 ± 0.5	14.0 ± 0.5
Tetracycline (MIC)	32	32	32	32
DMSO	-	-	-	-

View Article Online
DOI: 10.1039/C6RA02814D

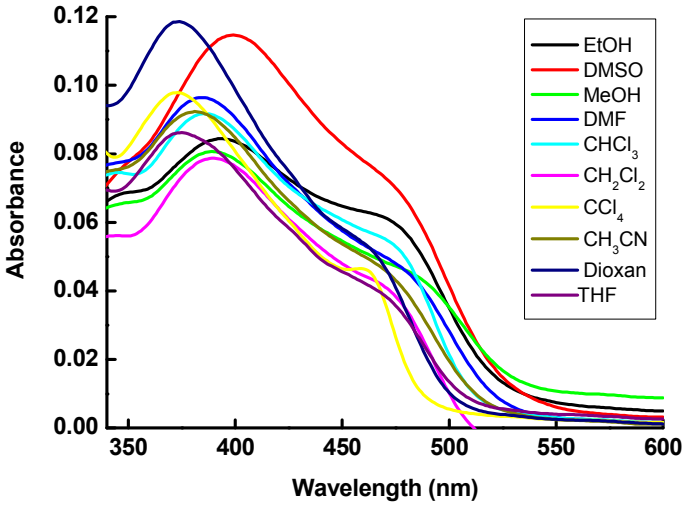

Fig.1- Electronic absorption spectra of 1 x 10^{-5} mol dm^{-3} of DDPC in different solvents.

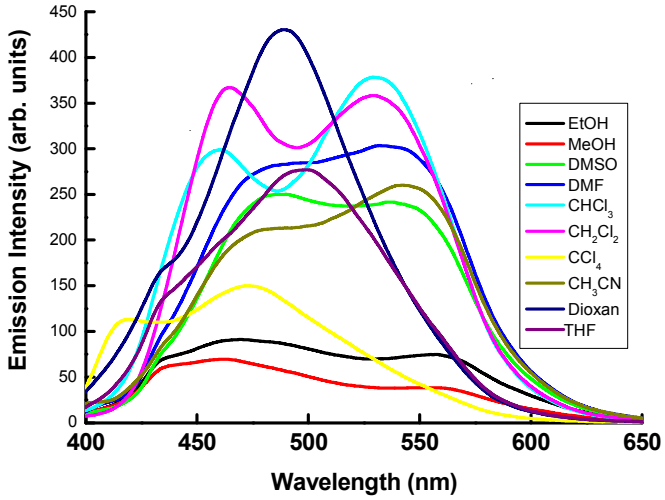

Fig.2- Emission spectra of 1 x 10^{-5} mol dm^{-3} of DDPC in different solvents (λ_{ex} = 385 nm)

View Article Online
DOI: 10.1039/C6RA02814D

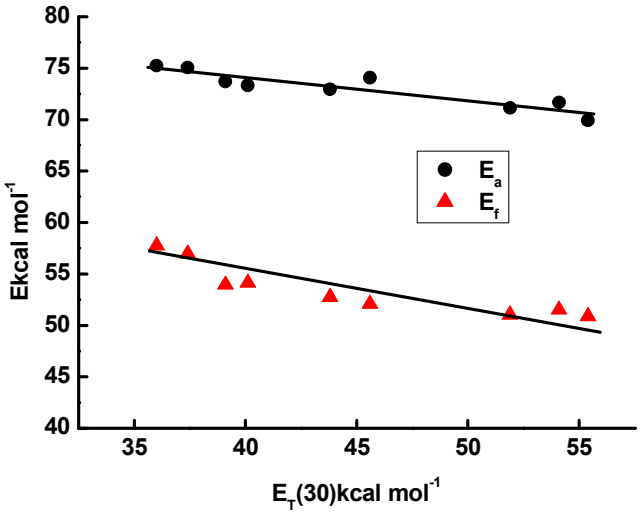

Fig.3- Plot of energy of absorption (E_a) and emission (E_f) versus $E_T(30)$ of different solvents

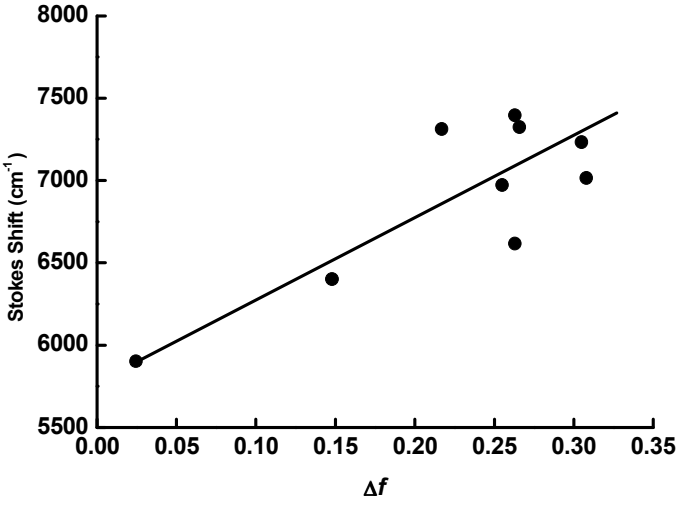

Fig.4- Plot Stokes shift ($\Delta\upsilon$) versus polarity (Δf) of solvent for DDPC

View Article Online
DOI: 10.1039/C6RA02814D

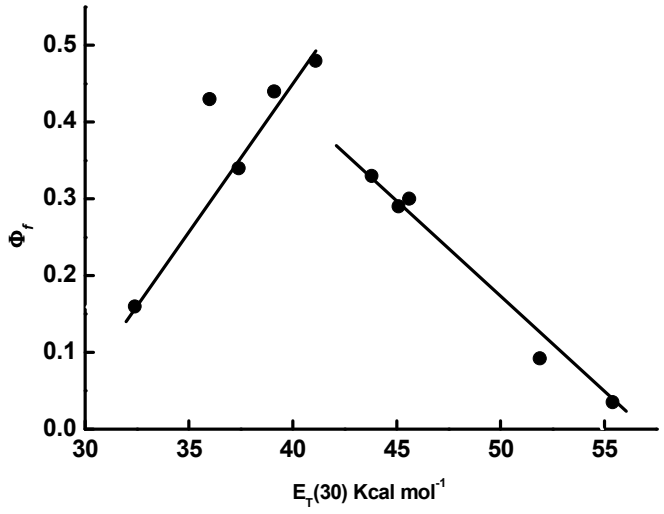

Fig.5- Plot of ϕ_f versus E_T (30) of different solvents

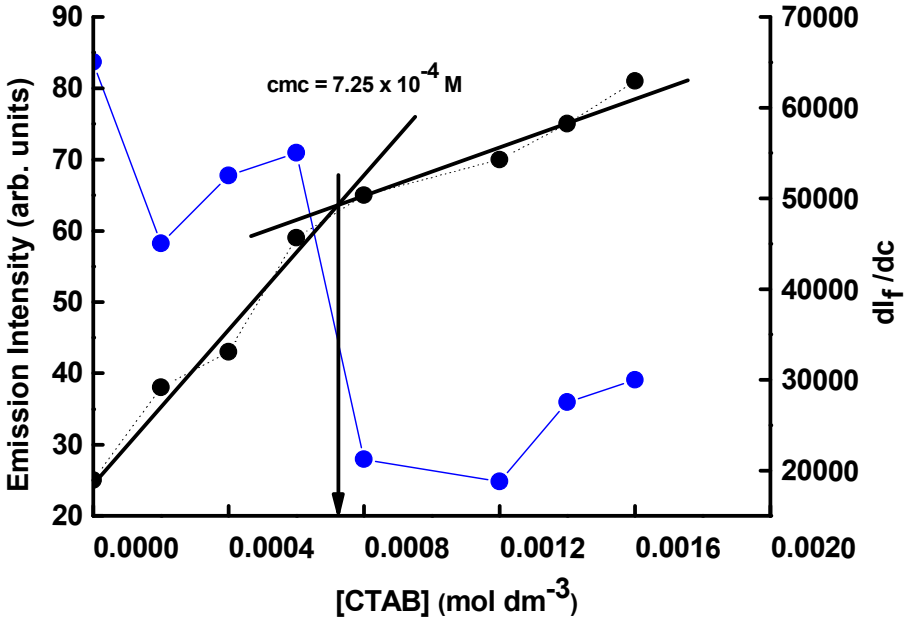

Fig.6- Plot of I_f versus the concentration of CTAB

View Article Online
DOI: 10.1039/C6RA02814D

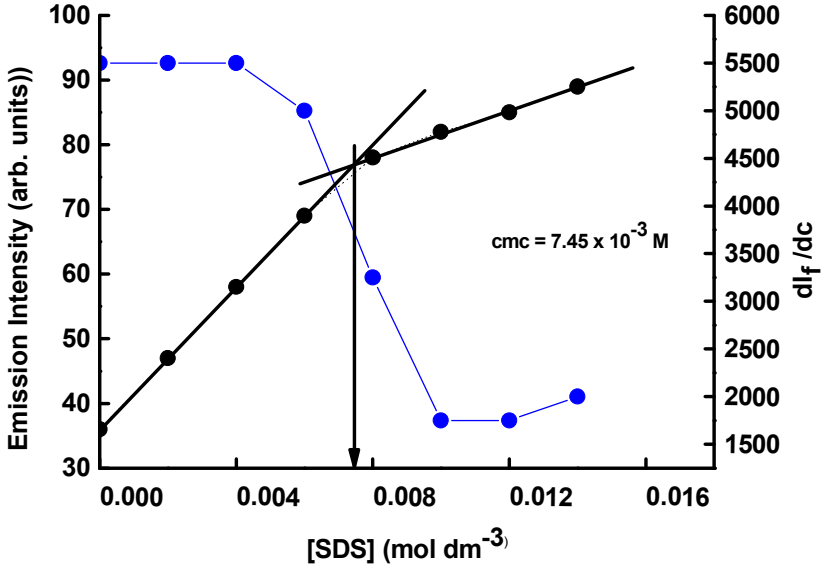

Fig.7- Plot of I_f versus the concentration of SDS

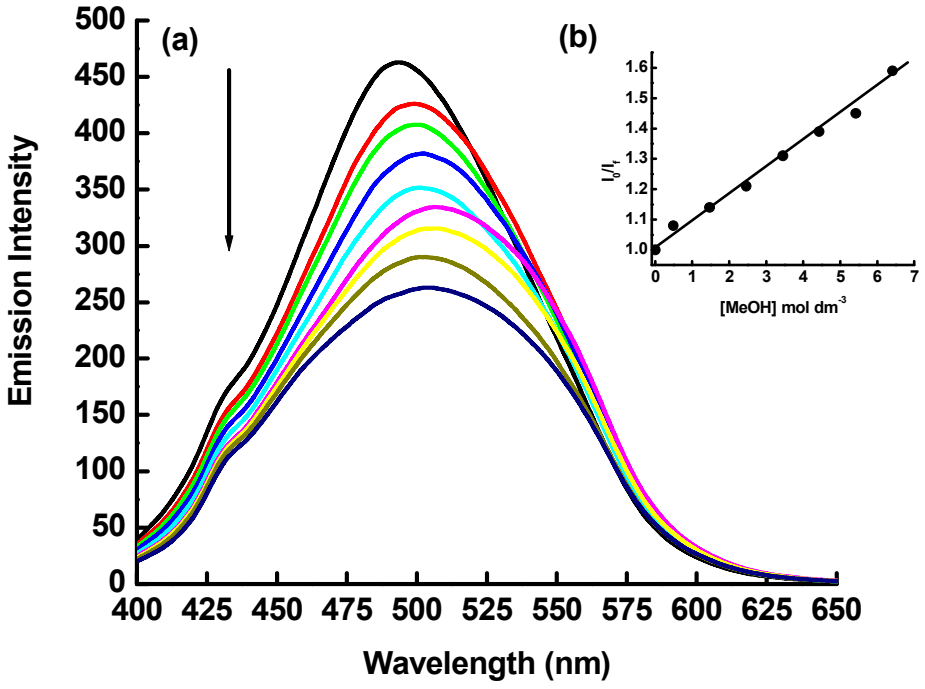

Fig. 8. (a) Fluorescence quenching of 1x10^{-5} mol dm^{-3} DDPC in dioxan (λ_{ex} = 385 nm) by MeOH, the concertration of MeOH at decreasing emission intensity are 0, 0.49, 1.47, 2.46, 3.45, 4.43, 5.43, 5.42, 6.41, 7.31 and 8.38 mol dm^{-3}. (b) Stern–Volmer plot of fluorescence quenching of 1x10^{-5} mol dm^{-3} of DDPC in dioxan by MeOH

View Article Online
DOI: 10.1039/C6RA02814D

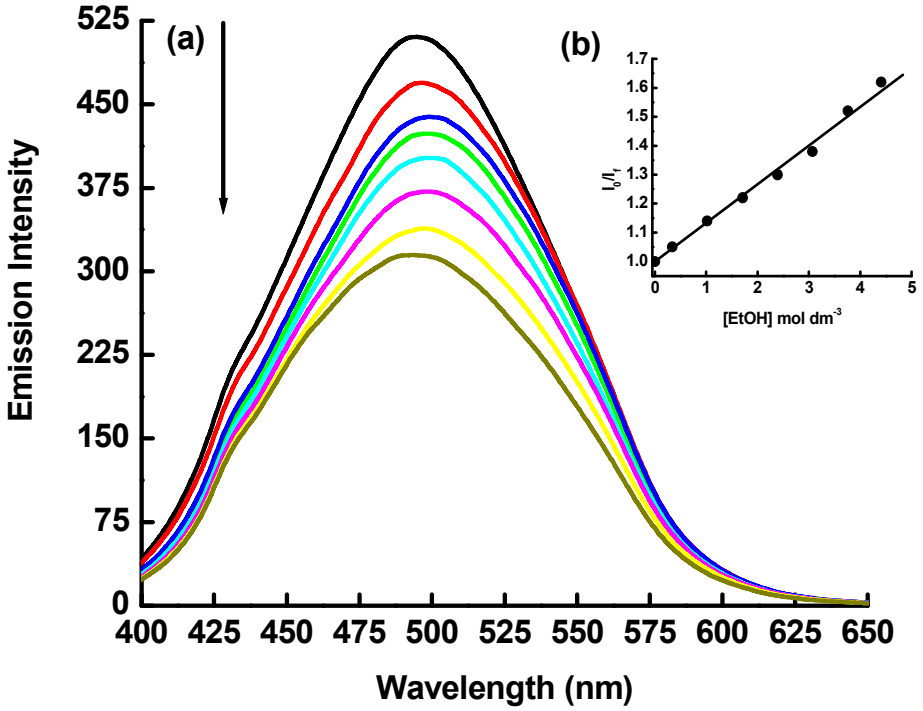

Fig. 9. (a) Fluorescence quenching of $1x10^{-5}$ mol dm^{-3} DDPC in dioxan (λ_{ex} = 385 nm) by EtOH, the concentration of EtOH at decreasing emission intensity are 0, 0.34, 1.02, 1.71, 2.39, 3.07, 3.76 and 4.44 mol dm^{-3}. (b) Stern–Volmer plot of fluorescence quenching of $1x10^{-5}$ mol dm^{-3} of DDPC in dioxan by EtOH

View Article Online
DOI: 10.1039/C6RA02814D

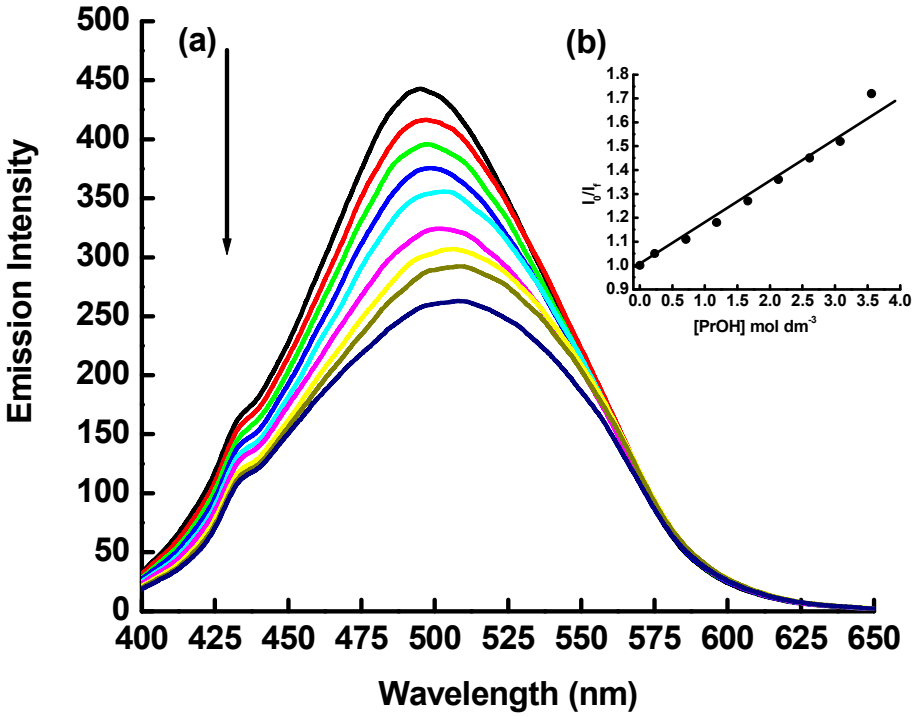

Fig. 10. Fluorescence quenching of $1x10^{-5}$ mol dm^{-3} DDPC in dioxan by (λ_{ex} = 385 nm) PrOH, the concentration of PrOH at decreasing emission intensity are 0, 0.23, 0.71, 1.18, 1.66, 2.13, 2.61, 3.08 and 3.56 mol dm^{-3} . (b) Stern–Volmer plot of fluorescence quenching of $1x10^{-5}$ mol dm^{-3} of DDPC in dioxan by PrOH

View Article Online
DOI: 10.1039/C6RA02814D

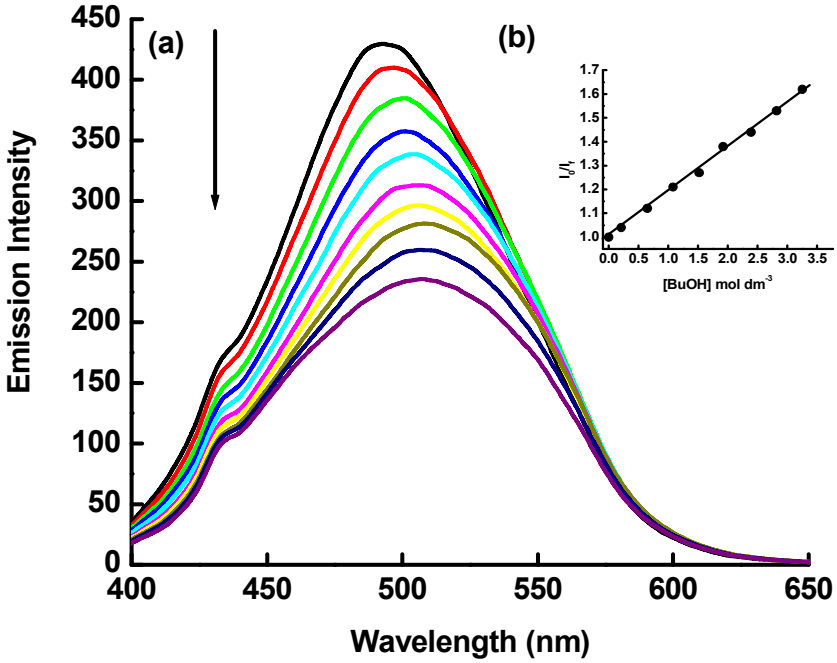

Fig. 11 (a). Fluorescence quenching of $1x10^{-5}$ mol dm^{-3} DDPC in dioxan (λ_{ex} = 385 nm) by BuOH, the concentration of BuOH at decreasing emission intensity are 0, .21, 0.65, 1.08, 1.52, 1.95, 2.39, 2.82 and 3.25 mol dm^{-3}. (b) Stern–Volmer plot of fluorescence quenching of $1x10^{-5}$ mol dm^{-3} of DDPC in dioxan by BuOH